The Open Access Journal of Science and Technology
vol. 7 (2019), Article ID 101265, 13 page
doi:10.11131/2019/101259

AgiAl Publishing House
http://www.agialpress.com/

Research Article

$TiO_2/FetiO_3/WO_3$ Ternary Composite Semiconductor as Efficient Photocatalyst: Structural Designing, Characteraization and Investigation of Photocatalytic Efficiency

Parvathy S[1], Saranya S[1] and Sivakumar S[2]

[1]*Department of Chemistry, Government Arts College, Salem-7, India*

[2]*Department of Chemistry, E. R. K Arts and Science College Dharmapuri-636905, India*

Abstract. WO_3, $FeTiO_3$ and TiO_2 photocatalyst prepared by simple sol-gel method followed by thermal treatment at 550°C, 550°C and 450°C for 3 hours respectively. $TiO_2/FeTiO_3/WO_3$ ternary composite has shown good activity for the degradation of reactive dyes in UV-visible light than that of binary composites such as TiO_2/WO_3, $TiO_2/FeTiO_3$. The prepared photocatalyst characterized by various techniques. 2 wt% $TiO_2/FeTiO_3/WO_3$ ternary composite has demonstrated highest activity for the degradation of Reactive Blue 160 (RB 160). The composite photocatalyst also has good reusability; the 2 wt% $TiO_2/FeTiO_3/WO_3$ photocatalyst completely degraded RB 160 in 120 minutes than that of parent photocatalysts. COD analysis of the degraded dye solution shows more than 70% of dye molecules in 100 mg l^{-1} reactive dye solution were mineralized in 3 hours. Hence, RB 160 photocatalyst will be an efficient and simplest method for the degradation of organic dyes and other organic pollutants in industrial effluent.

Keywords: Photocatalyst, sol-gel, composite, pollutants, dye

Corresponding Author

Parvathy S
paruchem70@gmail.com

Dates

Received 18 April 2019
Accepted 16 May 2019

1. Introduction

Textile effluent with unfixed dye molecules is the most important sources of water pollution [1,2]. Generally, wastewater containing organic dyes has enormous quantities of aromatic, which are found to be highly stable in nature. Conventional biological treatment methods are ineffective for the decolorization and mineralization of most of the organic dyes [3]. To minimize environmental problems due to the effluents containing residual dyes, efficient wastewater treatment technologies such as advanced oxidation processes (AOPs) and so on have been developed [4-6]. Heterogeneous photocatalysis is one of the important AOPs, which has been successfully used to oxidize many organic pollutants present in aqueous systems [7-9]. In this process semiconductors like TiO_2, ZnO, CdS, Fe_2O_3, etc., were used as photocatalyst for the mineralization of organic compounds to CO_2, water and mineral acids [10]. Photocatalytic activity was first popularized by the famous study of the 'Honda-Fujishima effect' on photoelectrochemical water splitting using a single-crystal titania electrode, which has been broadly used in many applications, including water cleavage, domestic and industrial

wastewater treatment, air cleaning, and self-cleaning surfaces. However, photocatalysis processes encounter low quantum efficiencies using traditional TiO_2 photocatalysts, which is the primary limitation of widely using sunlight energy. The band gap of TiO_2 (>3.0 eV) limits its light absorption to ultraviolet irradiation, which only constitutes approximately 4% of the solar spectrum, whereas visible light accounts for 43% and is the principal component of indoor artificial illumination, and only approximately 5% of radiation that reaches the earth contains UV light [11-16]. An effective and simple strategy to improve the photocatalytic activity of TiO_2 is constructing heterojunction with suitable semiconductors with a narrow band gap. These heterojunctions has great potential in tuning the electronic properties of the composite photocatalysts and efficient separation of photogenerated electron-hole pairs. However, the heterojunction of TiO_2 coupled with other narrow band gap semiconductors like CdS, V_2O_5, WO_3, Fe_2O_3, SeO_2 or $FeTiO_3$ increases its photocatalytic activity [17-25]. In addition, the lower efficiencies of traditional binary metal-oxide photocatalysts (e.g. TiO_2) are attributed to the high rate of electron-hole recombination after photo-assisted separation. In order to develop highly-active photocatalysts, second-generation visible-light sensitive photocatalysts of ternary metal oxides obtained via environmentally- friendly synthesis processes have increased in popularity recently. Approaches to improve photocatalytic efficiency and reusability have been studied, such as the development of Cadmium sulphide based and Iron titanate based visible-light-driven photocatalysts with lower band energies to enhance visible-light absorbance [26]. In $FeTiO_3$/TiO_2/WO_3, TiO_2 was sensitized by the $FeTiO_3$and WO_3in visible light, whereas in the ternary heterojunctions of wide band gap semiconductors such as TiO_2enhancement of photocatalytic activity was due to the separation of photogenerated electron-hole pair.

2. Materials And Method

This chapter deals with the method of preparation of doped and undoped photocatalyst, characterization techniques and the experimental setup used for the carrying out the photocatalytic degradation process

2.1 Chemicals Used

Reactive Blue160 a widely used in textile dye with two monochlorotriazine anchor groups supplied by Vexent dyeaux India Pvt. Ltd, Mumbai (Minimum dye content 70%) supplied by Loba Chemie India Pvt. Ltd, (Minimum dye content 90%) was used for photocatalytic degradation studies. Titanium tetrachloride (99%) and Ferrous Sulphate were supplied by Loba Pvt. Ltd; commercial tungstate (WO_3) was purchased Aldrich Pvt. Ltd; dye solutions for photocatalytic studies were prepared in double distilled water. Sodium hydroxide and hydrochloric acid (both AR grades from Qualigens) were used for modifying the pH of the solutions. Potassium dichromate (AR), Silver sulphate (GR), mercury sulphate (GR) 99% Ferroin (GR) and Sulphuric acid were used for COD analysis.

2.2 Synthesis of Photocatalysts

Synthesis of anatase TiO_2. All the photocatalysts was synthesized from $TiCl_4$ as reported elsewhere [27]. In the typical synthesis of TiO_2, 5 mL of $TiCl_4$ was added in 50 mL of ice cold

distilled water with stirring for 2 h and a clear solution was obtained after stirring, then to that solution, aqueous ammonia was added drop wise till the formation of a gel. The gel solution was washed repeatedly with distilled water to remove the entire chloride ions in the solutions and then it was kept for drying at 10°C to remove part of the absorbed water. The dry gel was milled and calcinated at 450°C for 4 h to obtain crystalline TiO_2.

Synthesis of $FeTiO_3$. In the Ilmenite $FeTiO_3$ synthesis, 2.5 mL of titanium tetrachloride was dissolved in 50 ml of ice cold distilled water. Separately, in another beaker 5.07 g of $FeSO_4.7H_2O$ was dissolved in 100 ml distilled water and then the solution was slowly added to the $TiCl_4$ solution with constant stirring. The pH of the mixture was adjusted to pH 8 by adding an aqueous ammonia drop wise until the formation of a gel. The gel was aged for 12 hours, then washed repeatedly with distilled water for the removal of chloride ions and followed by drying at 100°C to remove part of the absorbed water. The dry gel was the grounded into a fine powder in a pestle mortar and then calcinated at 550°C for 7 hours for the formation of $FeTiO_3$.

Preparation of $FeTiO_3/TiO_2$ heterojunction composite photocatalysts. In the preparation of 3 wt% $FeTiO_3/TiO_2$ heterojunction composites, 0.03 g of $FeTO_3$ was first dispersed in 40 ml of ethanol, to that suspension, 0.2750 g of oxalic acid was added, and the mixture was stirred in a magnetic stirrer to form a homogeneous suspension. To that suspension 0.97 g of TiO_2 was added, and the stirring was continued for 12 hours and then the suspension was dried and subsequently annealed at 300°C for 3 hours in a muffle furnace. The $FeTiO_3/TiO_2$ heterojunction composites with 1, 2, 3, 4 and 5 wt% of $FeTO_3$ were prepared by varying $FeTO_3$ and TiO_2 ratios as in a same method.

Preparation of WO_3/TiO_2 heterojunction composite photocatalysts. In the synthesis of 2 wt% WO_3/TiO_2 heterojunction composites, 0.02 g of WO_3 was first dispersed in 40 ml of ethanol, to that suspension, 0.2750 g of oxalic acid was added, and the mixture was stirred in a magnetic stirrer to form a homogeneous suspension. To that suspension 0.98 g of TiO_2 was added, and the stirring was continued for 12 hours and then the suspension was dried and subsequently annealed at 300°C for 3 hours in a muffle furnace. The WO_3/TiO_2 heterojunction composites with 4, 6, 8 and 10 wt% of WO_3 were prepared by varying WO_3 and TiO_2 ratios as in a same method.

Preparation of ternary composite photocatalysts: In the preparation of 0.5 wt% $FeTiO_3/TiO_2/WO_3$ ternary composites, 0.05 g of WO_3 and 0.995 g of $FeTiO_3/TiO_2$ was mixed with pistil mortar and ground gently to get fine powder. This ternary mixture subsequently annealed at 300°C for 3 hours in a muffle furnace. The $FeTiO_3/TiO_2/WO_3$ternary composites with 1, 2,3, 4 and 2.5 wt% of WO_3 were prepared by varying $FeTO_3/TiO_2$/and WO_3ratios as in a same method and labeled as FTW-1, FTW-2, FTW-3, FTW-4 and FTW-5 respectively.

2.3 Characterization of Photocatalyst

The powder X-ray diffraction patterns of the photocatalyst were recorded using Bruker AXS D8 Advance X-ray diffractometer with Cu-Kα radiation (λ=0.15406 nm) in the 2θ range 10° to 90° at room temperature. The surface morphology of the catalyst was analyzed using the scanning electron microscope JEOL Model JSM-6390LV. UV-Visible diffuse reflectance data were collected over the spectral range 200-800 nm with a Varian Cary-500 UV-Vis-NIR spectrometer equipped with an integrating sphere attachment and Gamma alumina was used as the reference material.

2.4 Photocatalytic Studies

All the photocatalytic experiments were performed under natural sunlight on clear sky days during the period of January to March-2019. In a typical experiment, 50 ml of dye solution (concentration 50 mg l^{-1}) was taken with 50 mg of photocatalyst in a 250-ml glass beaker. Then the dye solution was kept in direct sunlight with continuous aeration and the concentration of the dye remains was measured periodically by measuring its light absorbance at the visible λ_{max} by using Elico SL- 171 Visible spectrophotometer. In order to avoid the variation in results due to fluctuation in the intensity of the sunlight, a set of experiments has been carried out simultaneously. For pH studies the pH of the dye solutions was modified to different values (3, 5, 7, 9 and 12) by using 0.1 M HCl and NaOH solution.

Triazine dye Reactive Blue-160 (Figure 1) was used as a model pollutant to analyze the photocatalytic activity of nanocomposites.

Chemical formula: $C_{38}H_{23}C_{l2}N_{14}Na_5O_{18}S_5$

Molecular weight: 1309.85

CAS No: 71872-76-9 solar

λ_{max}: 616.

2.5 Intensity of Light

The potassium ferrioxalate actinometry developed by Hatchard and Parker was the most useful, solution-phase actinometer. The light intensity was measured as follows: Irradiate the appropriate actinometer solution in a photochemical reaction cell, whose volumes areV_1 (say 10 ml), for a period sufficient to produce a concentration of Fe^{2+} between 0.0005×10^{-6} and 3×10^{-6}mol/ml (usual irradiation time: 1-10 minute of irradiation is desirable). After irradiation for 't' seconds, and mixing well aliquot volumes, V (say, 5 ml) of the solution and a buffer solution of volume equal to about one-half volume of the photolytic (say, 2 ml) are added. After diluting it to volume, V_3 with water and mixing well, the solution is left without any disturbance for half an hour. All this operation is performed in the absence of actinometrical active light. Then an

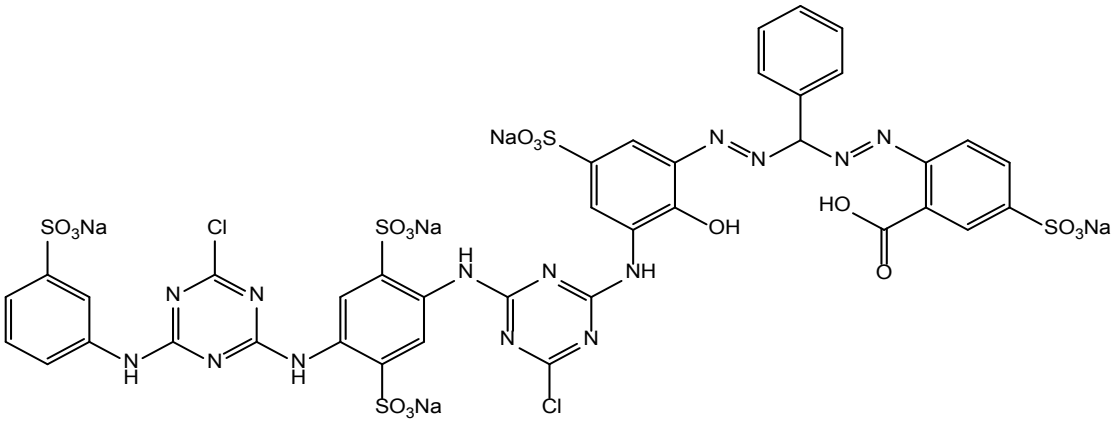

Figure 1: Structure of Reactive Blue-160.

identical but un-irradiated solution is prepared which is used as blank.

The Light intensity formula was given by,

$$Intensity\ of\ Sunlight,\ I\ \left(in\ Einstein\ s^{-1}cm^{-2}\right)=\frac{AV1V3}{\varepsilon d\Phi tV1a}$$

Where,

A=Absorbance (at 510 nm) of irradiation actinometer solution corrected for absorbance of blank.

D=Path length (in cm) of the absorption cell used in measurement of A.

E=Extinction coefficient of ferrous 1, 10 phenanthroline complex at 510 nm (=1.11 × 10^{-1} L $mol^{-1}cm^{-1}$).

Φ=Quantum yield of ferrous production.

V_1=Volume (in millilitre) of irradiated actinometer solution withdrawn.

V_2=Volume (in L) of actinometer solution irradiated.

V_3=Volumes (in millilitre) of volumetric flask used for dilution of irradiated liquid.

T=Irradiated time in minutes.

The intensity of sun light on all experimental days was measured by ferrioxalate actinometry and the average intensity of sunlight during the period of study was 4.7421 × 10^{-7} $Einsteins^{-1}cm^{-2}$.

3. Result and Discussion

3.1 XRD Pattern of Various Photocatalysts

XRD patterns of Pure $FeTiO_3$, WO_3, 3 wt% $FeTiO_3/TiO_2$ 4 wt% $WO_3/TiO_2$and 2 wt% $WO_{3/}$ $FeTiO_3/TiO_2$ ternary heterojunction, were given in the Figure 2. The XRD pattern indicates $FeTiO_3$, were in ilmenite (JCPDS No.75-1211) phase respectively. The diffraction patterns of TiO_2match the patterns in JCPDS card No. 21-1272, which indicating that TiO_2 was in pure anatase phase. The diffraction patterns of WO_3/TiO_2 and $FeTiO_3/TiO_2$heterojunctions are similar like the patterns of anatase TiO_2. The diffraction peak of $FeTiO_3$ and WO_3 were undetectable in the diffraction patterns of the FTW-2, this could be attributed to the high degree of dispersion of $FeTiO_3$ and WO_3 in the matrix of TiO_2 forming solid solution.

3.2 SEM Analysis

Scanning electron microscopic technique is used for the determination of morphologies and dispersion of the photocatalyst. Scanning electronic micrograph of $FeTiO_3/TiO_2$ and WO_3/TiO_2 heterojunctions was shown in Figure 3a and 3b. It consists of irregular agglomerated particles and in the form of bulky agglomerates. Figure 3c and 3d were shown the images of the $FeTiO_3/TiO_2$ and WO_3/TiO_2 heterojunctions respectively. From these micrographs Figure 3e $FeTiO_3/TiO_2/WO_3$photocatalysts dispersed in the form of small size irregular particles indicates that

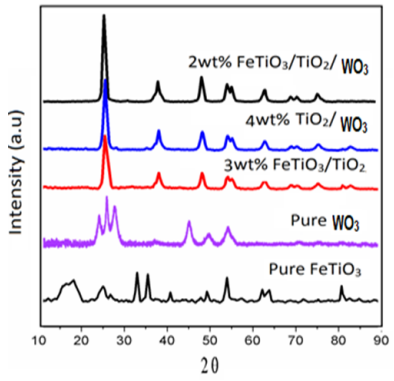

Figure 2: XRD patters of Pure $FeTiO_3$, WO_3, 3 wt% $FeTiO_3/TiO_2$ 4 wt% WO_3/TiO_2 and 2 wt% $WO_3/FeTiO_3/TiO_2$ ternary heterojunction.

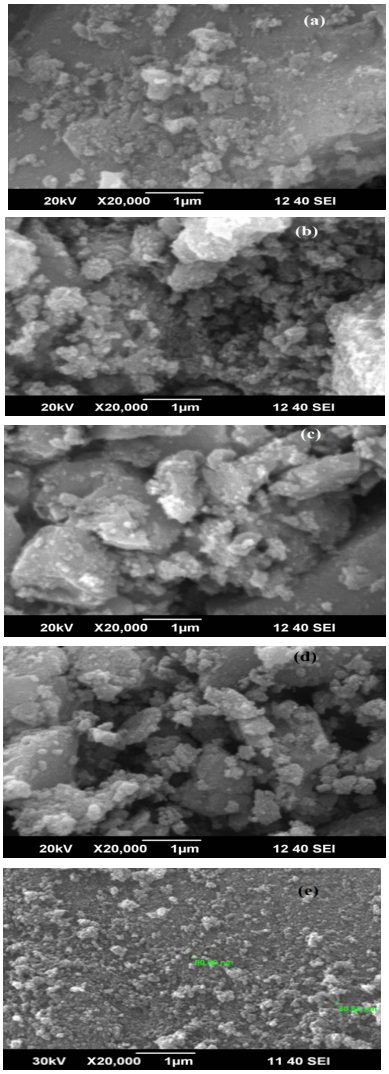

Figure 3: Shows the scanning electron micrographs of (a) $FeTiO_3$ (b) TiO_2 (c) $FeTiO_3/TiO_2$, (d) WO_3/TiO_2 and (e) 2 wt% $WO_3/FeTiO_3/TiO_2$ heterojunctions

WO_3 coupled with $FeTiO_3/TiO_2$photocatalyst.

3.3 DRS Analysis

The diffuse reflectance spectra of synthesized $FeTiO_3$, TiO_2, $FeTiO_3/TiO_2$, WO_3/TiO_2 and various types of $WO_3/FeTiO_3/TiO_2$are displayed in Figure 4**.** $FeTiO_3/TiO_2$ shows larger absorption than synthesized TiO_2in visible region; it reveals that increases the visible light activity of the catalyst. The ternary $WO_3/FeTiO_3/TiO_2$ also shifts to visible light absorption. This indicates coupling of narrow band gap semiconductors with TiO_2. To calculate the band gap energies of both catalysts, UV-visible spectra in the diffuse reflectance mode (R) were transformed to the Kubelka-Munk function F (R) to separate the extent of light absorption from scattering. The band gap energies of both catalysts were obtained from the plot of the modified Kubelka-Munk function (F (R) E) 1/2 versus the energy of the absorbed light E. The band gap energies of bare TiO_2 and $FeTiO_3/TiO_2$ and WO_3/TiO_2 are found to be 3.2 EV, 2.82 EV and 2.75 eV respectively.

3.4 Photocatalytic Studies

Photodegradability of reactive Blue160. The photocatalytic activity of the TiO_2, $FeTiO_3$, WO_3, $FeTiO_3/TiO_2$, WO_3/TiO_2 and $WO_3/TiO_2/FeTiO_3$ photocatalyst has been evaluated on reactive blue 160 (RB 160) in the presence of UV-visible light irradiation. This dye has been chosen for the studies since it has a strong light absorption in UV-visible region. The UV-visible transmittance spectrum of the RB 160 solution show that more than 80% of incident light in the wavelength range 200-450 nm was absorbed by 50 mg/l dye solution in a path length of 1 cm. Hence, the degradation of the RB 160 solution with concentration above 50 mg/l in a simple photocatalytic process over a UV active photocatalyst like TiO_2 is difficult and will take more treatment time for complete degradation.

The photocatalytic activity TiO_2 and $FeTiO_3/TiO_2$ photocatalyst were shown in Figure 5. The

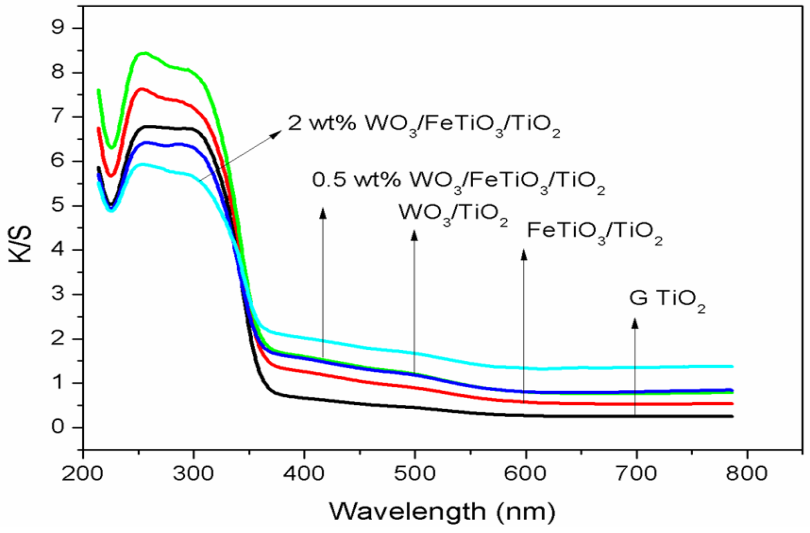

Figure 4: UV-visible diffused reflectance spectra of TiO_2, $FeTiO_3/TiO_2$, WO_3/TiO_2 and 2 wt% $FeTiO_3/TiO_2/WO_3$

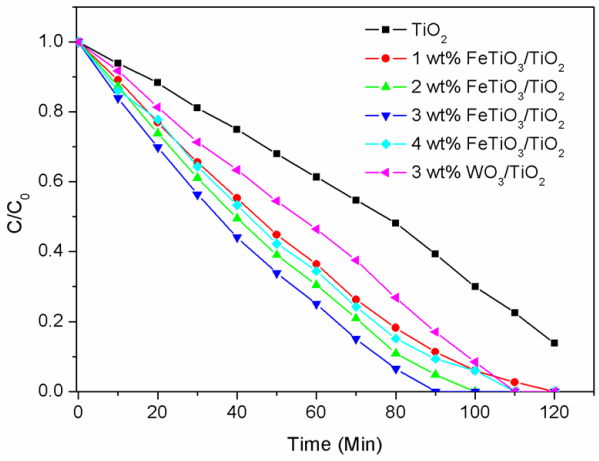

Figure 5: Photocatalytic degradation and kinetic plots of Reactive Blue160 over various photocatalysts.

photocatalytic activity of $FeTiO_3/TiO_2$ photocatalyst with different mass ratios exhibits better photocatalytic activity than that of bare TiO_2. It could be clearly seen that the photocatalytic degradation rate of RB 160 was gradually increased with increase of $FeTiO_3$ content, which indicated that RB 160 could be degraded more efficiently by $FeTiO_3$ coupled with TiO_2than that of TiO_2. It was interesting to note that the 3 wt% $FeTiO_3/TiO_2$ exhibited the highest photocatalytic degradation efficiency. But at the higher $FeTiO_3$ content, the photocatalytic activity decreased, suggesting that the optimal $FeTiO_3$ on TiO_2existed when the weight ratio was 3%.

The photocatalytic activity TiO_2 and WO_3/TiO_2 photocatalyst were shown in Figure 6. The photocatalytic activity of WO_3/TiO_2 photocatalyst with different mass ratios exhibits better photocatalytic activity than that of bare TiO_2. It could be clearly seen that the photocatalytic degradation rate of RB 160 was gradually increased with increase of WO_3 content, which indicated that RB 160 could be degraded more efficiently by WO_3 coupled with TiO_2 than that of TiO_2. It was interesting to note that the 3 wt% WO_3/TiO_2 exhibited the highest photocatalytic degradation efficiency. But at the higher WO_3 content, the photocatalytic activity decreased, suggesting that the optimal WO_3 on TiO_2 existed when the weight ratio was 3%.

Further the photocatalytic study has been extended to improve the photocatalytic efficiency of TiO_2. This result exhibited in Figure 7a, photocatalytic activities of the various weight ratios of WO_3 on $FeTiO_3/TiO_2$ heterojunctions in the presence of UV-visible light irradiations. In this study, the optimized 3 wt% $FeTiO_3/TiO_2$ heterojunctions coupled with WO_3 at various weight ratios. After 60 min of UV-visible illumination, the RB 160 degrades over WO_3 and 3 wt% $FeTiO_3/TiO_2$heterojunctions are only 30% and 67%, respectively. However, WO_3/3 wt%$FeTiO_3$/TiO_2 the heterojunctions composites show the higher photocatalytic degradation rate (71–99%) in the presence of same experimental conditions. It is worth noting that WO_3/3 wt%$FeTiO_3/TiO_2$ heterojunctions composites could be inducing notable photodegradation efficiency from 70% to 99% beyond the increases of 4 wt% WO_3/3 wt%$FeTiO_3/TiO_2$ heterojunctions composites. This shows that the photocatalytic activity of WO_3/3 wt% $FeTiO_3/TiO_2$ heterojunctions composites increases with the increase in WO_3 content upto 4 wt%. Further increases the WO_3 content, the photocatalytic efficiency were slightly decreased (90%). As a result, 4 wt% of WO_3 is the optimum dosage ratio in the WO_3/3 wt%$FeTiO_3/TiO_2$ heterojunctions composites.

The photocatalytic degradation kinetics of RB 160 was investigated under the influence of

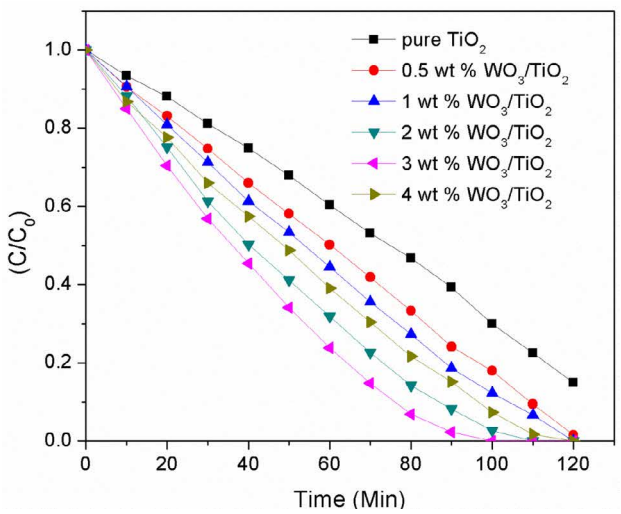

Figure 6: Photocatalytic degradation of Reactive Blue160 over WO_3/TiO_2 heterojunction photocatalysts.

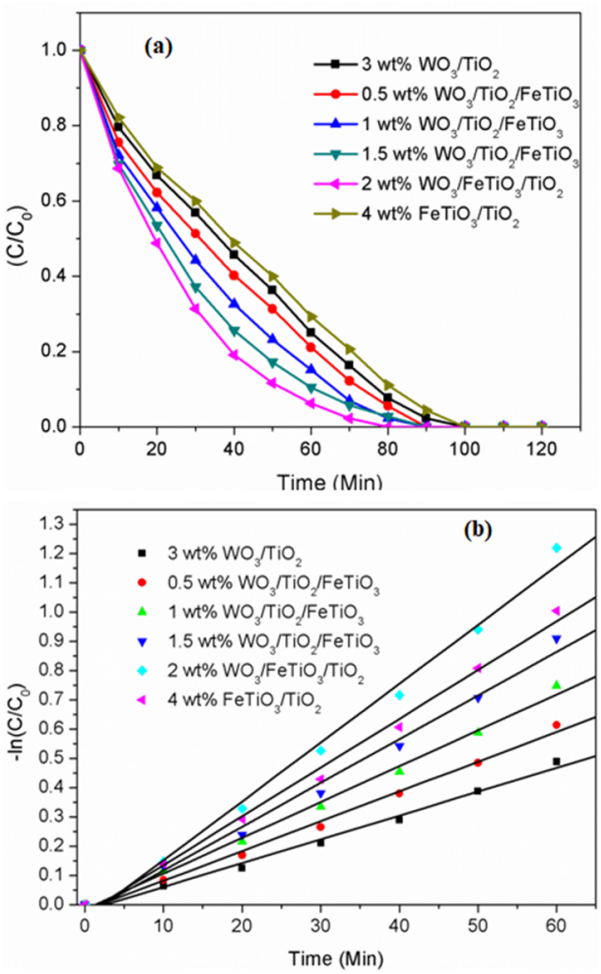

Figure 7: (a and b) Photocatalytic degradation and kinetic plots of Reactive Blue 160 over various photocatalysts.

WO_3/3 wt%$FeTiO_3$/TiO_2 heterojunctions composites were shown in Figure 7b.

The data obtained from the degradation studies were analyzed with the Langmuir–Hinshelwood kinetic model:

$$r_s = \frac{kKc}{1+KC}$$

where r_S is the specific degradation reaction rate the dye ($mgl^{-1}min^{-1}$), C the concentration of the dye (mgl^{-1}), k the reaction rate constant (min^{-1}) and K is the dye adsorption constant. When the concentration (C) is small enough, the above equation can be simplified in an apparent first-order equation:

$$r_s = kKC = K_{app}C\left(=-\frac{dc}{dt}\right)$$

After integration, we will get

$$-In\left(\frac{C}{C_0}\right) = k_{app}t$$

where C_0 is the initial concentration ($mg\ l^{-1}$), C is the concentration of the dye after (t) minutes of illumination. The data obtained from the degradation of RB 160 fits well the apparent first order kinetics (Figure 7b). The electrons in the conduction band can be transferred to surface adsorbed oxygen molecules and form superoxide anions, which can further transform to $OH^{\bullet}$ and initiate the degradation of RB 160.

Photocatalytic mechanism. The work mechanism of this nanocomposite is illustrated in Figure 8. As shown in Figure 8, $FeTiO_3$ as an electron acceptor can prevent the e- and h_+ from recombination in the UV-visible photoexcitation of TiO_2. This function of $FeTiO_3$ can promote the decomposition of organic pollutants by the oxidation of the h+. The applications conversing this principle, namely organic compounds as the h+ scavenger for the elimination of selenite pollutants, have been extensively studied. Then, $FeTiO_3$, can deposit onto TiO_2 and shift the

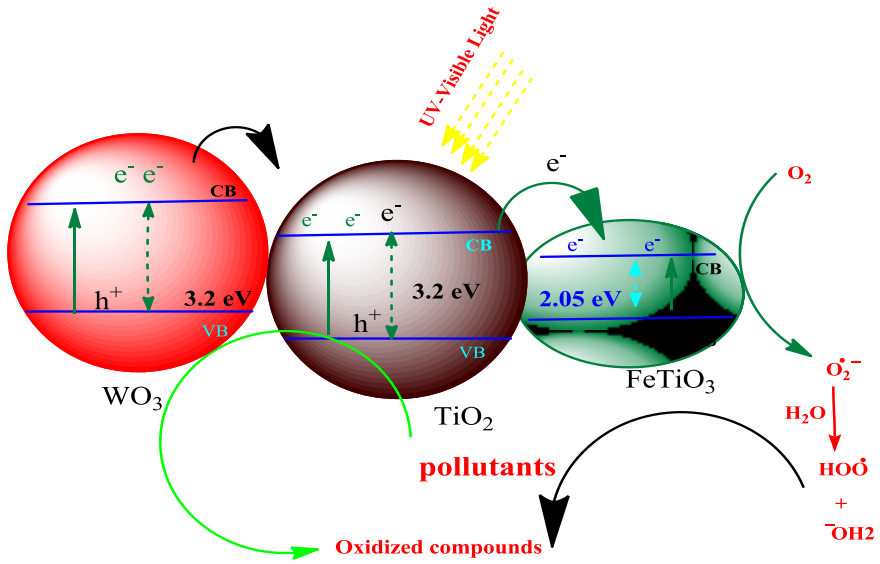

Figure 8: Photocatalytic mechanism of prevention of electron-hole recombination and electron injection process of 2 wt% WO_3/$FeTiO_3$/TiO_2.

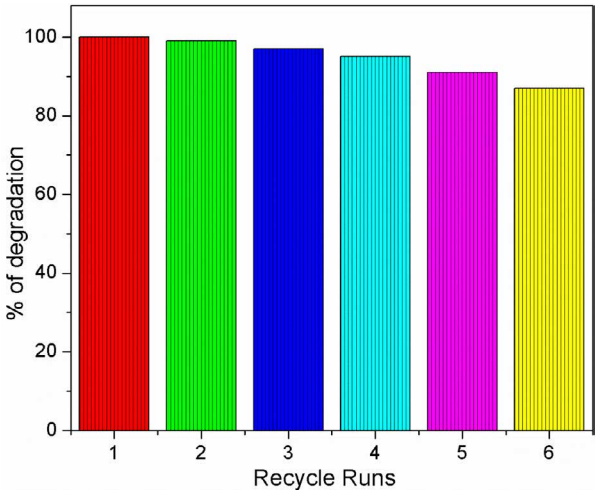

Figure 9: Reusability of 2 wt% $WO_3/FeTiO_3/TiO_2$.

absorbency of the system to the visible light region due to $FeTiO_3$ narrow band gap (2.0 eV). In addition, when illuminated, Cd Scan donates the electron and have been used to degrade organic dye.

Furthermore, the combination of WO_3, TiO_2 and $FeTiO_3$ in which the photocurrent is produced by transferring e^- from TiO_2 to $FeTiO_3$ when exposed to visible light. This process can also prevent the e^- and h^+ from recombination.

Finally, it is worthy of pointing out that the transformation from $FeTiO_3$ is possible by photo-oxidizing, which make the $FeTiO_3$ in system un-losing. Thus, the 3 wt% $FeTiO_3/TiO_2/WO_3$ system is a hopeful form of further improving the practicability of WO_3 and TiO_2.

Reusability of the photocatalyst. Reusability is a very important parameter in assessing the practical application of photocatalysts in wastewater treatment. It can contribute significantly to lowering the operational cost of the process. Hence the reusability of the 2 wt% $WO_3/FeTiO_3/TiO_2$ ternary composites was studied for the degradation of 100 mg l^{-1} RB 160 solution at pH 3. The photocatalyst was carefully separated from the degraded dye solution by centrifugation and added to the fresh 100 ml dye solution. The results of the analysis were shown in Figure 9. It has been found that 2 wt% $WO_3/FeTiO_3/TiO_2$ ternary composites completely degraded the RB 160 solution in 120 minutes, even in its third reuse; this shows that the composites have good stability in the acidic conditions. Hence application of 2 wt% $WO_3/FeTiO_3/TiO_2$ ternary composites for the treatment of textile effluents will be cost effective.

4. Conclusion

Heterojunction composites such as WO_3/TiO_2, $FeTiO_3/TiO_2$ and ternary $WO_3/FeTiO_3/TiO_2$ was prepared in a simple dispersed method from the metal oxides synthesized by sol-gel method. The synthesized photocatalysts have been evaluated from their activity in the degradation of Reactive Blue 160 in the presence of UV-visible light. From the degradation result, $WO_3/FeTiO_3/TiO_2$ ternary composites showed higher photocatalytic activity than that of $FeTiO_3/TiO_2$ and WO_3/TiO_2 heterojunctions shows the favourable photocatalytic activity at pH 3. The mineralization of reactive dyes with triazine groups has been reported to be more difficult in most treatment

methods. However, at higher concentrations, the dye solutions, especially chlorotriazine dye solutions transmit only very small portion of photons to reach the photocatalyst surface. Further the $WO_3/FeTiO_3/TiO_2$ ternary composites were also used for the degradation of four other reactive dyes with different functional groups.

5. References

1. W. Z. Tang and A. Huren. "Photocatalytic degradation kinetics and mechanism of acid blue 40 by TiO_2/UV in aqueous solution". *Chemosphere*, Vol. 31, pp: 4171-4183, 1995.
2. M. Saquib and M. Muneer. "TiO_2-mediated photocatalytic degradation of a triphenylmethane dye (gentian violet), in aqueous suspensions". *Dyes Pigm*, Vol: 56, pp: 37-49, 2003.
3. S. Adishkumar and S. Kanmani. "Treatment of phenolic wastewaters in a single baffle reactor by solar/TiO_2/H_2O_2 process". *Desalination Water Treat*, Vol: 24, pp: 67-73, 2010.
4. A. N. Rao, B. Sivasankar and V. Sadasivam. "Kinetic studies on the photocatalytic degradation of direct yellow 12 in the presence of ZnO catalyst". *J Mol Catal A: Chem*, Vol: 306, 77-81, 2009.
5. Z. S. Seddigi. "Removal of Alizarin yellow dye from water using zinc doped WO_3 catalyst". *Bull Environ Contam Toxicol*, Vol: 84, pp: 564-567, 2010.
6. M. A. Rauf and S. S. Ashraf. "Radiation induced degradation of dyes-An overview". *J Hazard Mater*, Vol: 166, pp: 6-16, 2009.
7. V. Stengl, F. Oplustil and T. Nemec. "In^{3+}-doped TiO_2 and TiO_2/In_2S_3 Nanocomposite for photocatalytic and stoichiometric degradations". *Photochem Photobiol*, Vol: 88, pp: 265-276, 2012.
8. N. Neelakandeswari, G. Sangami, N. Dharmaraj, N. K. Taek and H. Y. Kim. "Spectroscopic investigations on the photodegradation of toluidine blue dye using cadmium sulphide nanoparticles prepared by a novel method". *Spectrochim Acta - Pt A: Mol Biomol Spectrosc,* Vol: 78, pp: 1592-1598, 2011.
9. B. Esen, T. Yumak, A. Sinağ and T. Yildiz. "Investigation of photocatalytic effect of SnO_2 nanoparticles synthesized by hydrothermal method on the decolorization of two organic dyes". *Photochem Photobiol, Vol:* 87, pp: 267-274, 2011.
10. M. Stylidi, D. I. Kondarides and X. E. Verykios. "Visible light-induced photocatalytic degradation of acid orange 7 in aqueous TiO_2 suspensions. *Appl Catal B,* Vol: 47, pp: 189-201, 2004.
11. B. Krishnakumar and M. Swaminathan. "Influence of operational parameters on photocatalytic degradation of a genotoxic azo dye acid violet 7 in aqueous ZnO suspensions". *Spectrochim Acta-Pt. A: Mol Biomol Spectrosc*, Vol: 81, pp: 739-744, 2011.
12. M. Anheden, D. Y. Goswami and G. Svedberg. "Photocatalytic treatment of wastewater from 5-fluorouracil manufacturing". *J Solar Energy Eng Trans* ASME, Vol: 118, pp: 2-8, 1996.

13. D. F. Ollis, E. Pelizzetti and N. Serpone. "Destruction of water contaminants". *Environ Sci Technol,* Vol: 25, pp: 1523-1529, 1991.

14. J. Gao, X. Luan, J. Wang, B. Wang, K. Li, Y. Li, P. Kang and G. Han. "Preparation of Er^{3+}: $YAlO_3$/Fe-doped TiO_2–ZnOand its application in photocatalytic degradation of dyes under solar light irradiation". *Desalination*, Vol: 268, pp: 68-75, 2011.

15. L. R. Hou, C. Z. Yuan and Y. Peng. "Synthesis and photocatalytic property of SnO_2/ TiO_2nanotube composites". *J. Hazard. Mater*, Vol: 139, pp: 310-315, 2007.

16. J. C. Trist~ao, F. Magalh~aes, P. Corio and M. T. C. Sansiviero. "Electronic characterization and photocatalytic properties of CdS/TiO_2 semiconductor composite". *J Photochem Photobiol A*, Vol: 181, pp: 152-157, 2006.

17. S. A. K Leghari, S. Sajjad, F. Chen and J. Zhang. "WO_3/ TiO_2 composite with morphology change via hydrothermal templatefree route as an efficient visible light photocatalyst". *Chem Eng J,* Vol: 166, pp: 906-915, 2011.

18. M. Sun, G. Chen, Y. Zhang, Q. Wei, Z. Ma and B. Du. "Efficient degradation of azo dyes over Sb_2S_3/TiO_2heterojunction under visible light irradiation". *Ind Eng Chem Res,* Vol: 51, 2897-2903, 2011.

19. Y. Bessekhouad, D. Robert and J. V. Weber. "Bi_2S_3/TiO_2 and CdS/TiO_2 heterojunctions as an available configuration for photocatalytic degradation of organic pollutant". *J Photochem Photobio,* Vol: 163, 569-580, 2004.

20. L. Shi, C. Li, H. Gu and D. Fang. "Morphology and properties of ultrafine SnO_2-TiO_2 coupled semiconductor particles". Mater Chem Phys, Vol: 62, 62-67, 2000.

21. A. Chakraborty and M. Kebede. "Efficient decomposition of organic pollutants over In_2O_3/ TiO_2nanocompositephotocatalyst under visible light irradiation". *J Cluster Sci*, Vol: 23, pp: 247-257, 2012.

22. M. E. Zorn, D. T. Tompkins, W. A. Zeltner and M. A. Anderson () Photocatalytic oxidation of acetone vapor on TiO_2/ZrO_2 thin films. *Appl Catal B,* Vol: 23, pp: 1-8, 1999.

23. C. Gao, J. Li, Z. Shan, F. Huang and H. Shen. "Preparation and visible-light photocatalytic activity of In_2S_3/TiO_2 composite". *Mater Chem Phys*, Vol: 122, pp: 183-187, 2010.

24. Y. J. Kim, B. Gao, S. Y. Han, M. H. Jung, A. K. Chakraborty, T. Ko, C. Lee and W. I. Lee. "Heterojunction of $FeTiO_3$nanodisc and TiO_2 nanoparticle for a novel visible light photocatalyst". *J Phys Chem C*, Vol: 113, 19179-19184, 2009.

25. M. Logar, A. Kocjan and A. Dakskobler. "Photocatalytic activity of nanostructured c-Al_2O_3/ TiO_2 composite powder formed via a polyelectrolyte-multilayer-assisted sol-gel reaction". *Mater Res Bull,* Vol: 47, 12-17, 2012.

26. S. B. Rawal, A. K. Chakraborty and W. I. Lee. "Heterojunction of FeOOH and TiO_2 for the formation of visible light photocatalyst". *Bull Korean Chem Soc*, Vol: 30, pp: 2613-2616, 2009.

27. J. Yuan, M. Chen, J. Shi and W. Shangguan. *Int J Hydr Ener*, Vol: 3, pp: 1326-1331, 2006.